

## Ground-Penetrating Radar for Studies of Peatlands in Permafrost

M.S. Sudakova<sup>a,b,✉</sup>, M.R. Sadurtdinov<sup>a</sup>, A.M. Tsarev<sup>a</sup>, A.G. Skvortsov<sup>a</sup>, G.V. Malkova<sup>a</sup>

<sup>a</sup> Earth Cryosphere Institute, Tyumen Scientific Center, Siberian Branch of the Russian Academy of Sciences,  
ul. Malygina 86, Tyumen, 625026, Russia

<sup>b</sup> M.V. Lomonosov Moscow State University, Leninskie Gory 1, Moscow, 119234, Russia

Received 16 March 2018; accepted 17 September 2018

**Abstract**—Ground-penetrating radar (GPR) profiling is applicable to study peatlands and swampy areas in permafrost but have some limitations in summer time. Theoretical calculations and field experiments show that estimating attenuation of electromagnetic waves is required for planning GPR survey. GPR data acquired with a 300 MHz antenna fail to resolve reflections from below the permafrost if the thaw/permafrost boundary is deeper than 1.5 m and the attenuation coefficient is 0.7, as in water-saturated peat. GPR data allow high-resolution lithological division of permafrost and provide reliable constraints on the depths to interfaces and physical properties of the ground. Thus, GPR can fully or partly substitute for the time- and labor-consuming direct measurements. The inferences have been confirmed by field results.

**Keywords:** GPR, dynamic parameters, attenuation, volumetric water content

### INTRODUCTION

Preservation of carbon deposits (peat) in paludal and forest ecosystems is among top priorities of geoenvironment research in the Arctic. The Arctic ecosystems store great amounts of carbon which maintains global-scale climate stability (Konchits and Minaeva, 2017). Peat is a heat insulator that prevents permafrost from degradation and, on the other hand, is a potential energy source (local fuel). The interest to local energy resources as a cheaper alternative to imported fuels has increased lately (Power Economy of Russia, 2009; Malygin and Lubov, 2014; Timofeeva and Mingaleeva, 2014). West Siberia is the world largest peat basin where peat thickness locally reaches 8–10 m (Vasil'chuk and Vasil'chuk, 2016; Fotiev, 2017).

Peat deposits pose environment risks being prone to spontaneous ignition in hot and dry weather and to prolonged burning with release of abundant carbon dioxide. To avoid disastrous fire consequences, special monitoring is required in paludal ecosystems (vegetation and peatlands of different thicknesses and origin).

Studies of swampy areas in permafrost include measurements of depths to the peat base and to the permafrost table. These depths can be successfully determined using ground-penetrating radar (GPR): sounding the subsurface with high-frequency (10 MHz–3 GHz) electromagnetic signals. GPR data can be used to (1) detect anomalies, interfaces, and local objects; (2) estimate depths to interfaces and sizes of objects/

anomalies; (3) characterize (qualitatively or quantitatively) mechanic or electromagnetic properties of the ground. Obviously, detection of objects (1) should precede depth estimation (2), and both are indispensable for solving problem (3).

GPR data allow mapping the thaw/permafrost interface, except for the case of clayey or saline active layer (Omeliyanenko, 2001; Brosten et al., 2009; Ermakov and Starovoitov, 2010; Shean and Marchant, 2010; Starovoitov, 2008; Sadurtdinov et al., 2016; Sudakova et al., 2017), as well as the peat/mineral soil interface (Plado et al., 2011; Rosa et al., 2009). Both interfaces are strong reflectors and the reflections are prominent against noise. However, reflections from the peat base lying below the permafrost table may be poorly resolvable in GPR data. The published reports of successful GPR imaging of the peat/soil interface (Sjöberg et al., 2015) only refer to the cases when it is above the permafrost table. When interpreting GPR data from permafrost peat sections, it is important to take into account attenuation of electromagnetic waves and presence/absence of reflections from the peat base located below the permafrost table.

The depths to interfaces and objects are commonly evaluated by tying geophysical data to core sections and by calculating EM (electromagnetic) velocities from diffraction hyperbolas or from *a priori* data (Starovoitov, 2008; Vladov and Sudakova, 2017). Thus obtained velocity values are extrapolated over the whole survey area or over profiles reaching hundreds of meters or even a few kilometers, but the true velocities may vary within short distances. For instance, we witnessed a change from 3.5 to 7.0 cm/ns within 100 m (Sudakova et al., 2017). The accuracy of depth estimates can be improved using WARR (wide-angle reflection and refraction) measurements.

✉ Corresponding author.

E-mail address: m.s.sudakova@yandex.ru (M.S. Sudakova)

Velocities inside layers of lithologically uniform deposits can be recalculated to soil moisture via known empirical correlation relationships (Butler, 2005). Soil moisture is commonly measured directly, by the gravimetric measurements, in samples from small specially dug pits (Pavlov and Malkova, 2009). The water content values obtained at some points are assigned to the whole active layer, which is fraught with errors increasing proportionally to the active layer thickness. Moreover, these measurements are time and labor consuming. The space and time variations of soil moisture are related with dielectric permittivity and thus can be measured and monitored by GPR.

Our investigation demonstrates applicability of GPR in the swampy areas and peatlands that differ in origin and peat thickness, in the upper reaches of the Pechora River (Nenets Autonomous District).

## INSTRUMENTS AND METHODS

The studies were carried out along profiles in different landscapes (Fig. 1), in the ground consisting of frozen or unfrozen peat, sand and silt of different thicknesses. The field work included GPR sounding, coring, and direct measurements of active layer thickness with a metal rod.

GPR data were acquired by continuous profiling using a RadarSystems Zond-12e system (Riga, Latvia) with shielded bow-tie antennas antennas of 150 and 300 MHz center frequencies (Fig. 2a). The sampling rate, number of counts, and acquisition time were chosen according to specific objectives and geocryological conditions. The measurement points (traces or A-scans) were spaced at 2 to 5 cm. The profiles were referenced with GPS and tape measurements at key points (every 10–25 m). EM velocities were estimated at selected points of the profiles by WARR. We use continuous sounding with a receiver antenna pulled relative to fixed source antenna.

The acquired data were processed using the *Radexplorer* and *RadexPro* software (*Dekogeofizika SK*, Moscow, Russia). The processing flow included scaling of GPR data against markers; zero offset correction; bandpass filtering

(Ormsby filter) in the signal band; spherical divergence correction; and estimating the velocities of EM waves.

The depths to interfaces and their nature inferred from GPR were checked against coring data. Boreholes were made by pressure coring with a portable drilling rig (Fig. 2b) to depths reaching the peat base and the permafrost table with reference to presumed depths to these interfaces.

## ATTENUATION OF ELECTROMAGNETIC WAVES IN PEAT

The dynamic range in conventional radars does not exceed that of the built-in ADC (analog-to-digital converter). For a 16-bit ADC, the maximum to minimum signal range is about 90 dB but it may reduce to 70 dB at the maximum signal-to-instrument noise ratio about 5000. In the reported surveys, the relative amplitudes were about  $10^4$  for the transmitted signal and within 10 for noise, i.e., the dynamic range was from 60 to 80 dB. To check the possibility for detection of deep reflections, the dynamic range was assumed to be 70 dB, which is typical of standard radars (Harry, 2009); the amplitude reduction of waves penetrating through the target medium and reflected from the target interface should be within 70 dB.

In order to estimate the possibility for picking reflections from below the permafrost table in GPR data, some calculations are required, with assumptions common in the GPR practice.

According to the classical theory, the amplitude  $A_h$  of a signal propagating in a uniform ground and reflected from an interface at the depth  $h$  is

$$A_h = A_0 K_{\text{ref}} \prod_{i=1}^n (1 - K_{i\text{ref}}^2) \cdot e^{-2h \cdot \alpha} \cdot \frac{1}{2h}, \quad (1)$$

where  $A_0$  is the amplitude of the initial (sounding) signal;  $K_{\text{ref}}$  is the reflection coefficient at the depth  $h$ ;  $\prod_{i=1}^n (1 - K_{i\text{ref}}^2)$  is the dot product of the transmission coefficients through

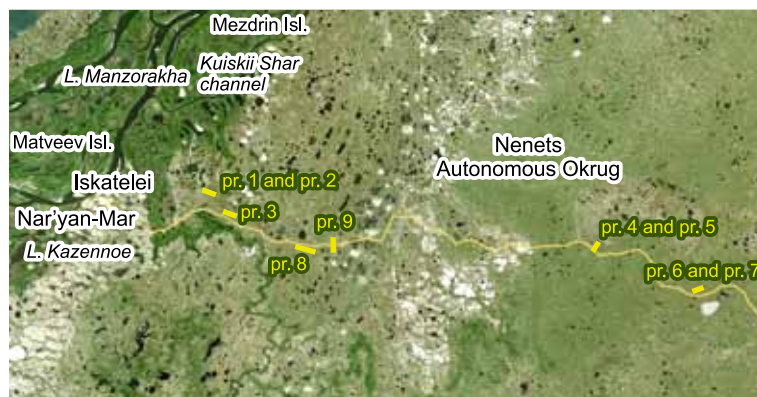


Fig. 1. Location map of study area along the Nar'yan-Mar–Shapkina profile.



Fig. 2. GPR profiling (a) and coring (b) in the study area.

intermediate boundaries and back;  $e^{-2h\alpha} \cdot \frac{1}{2h}$  is the attenuation and divergence of a spherical wave.

A water-saturated peat section in permafrost can be simulated by two simple layered models (Fig. 3): the thaw/permafrost interface below (model 1) or above (model 2) the peat/mineral interface. The coefficients  $K_{ref}$  of reflection from the interfaces are

$$K_{ref} = \frac{v_2 - v_1}{v_2 + v_1} \quad (2)$$

Average velocities in unfrozen water-saturated peat and sand are, respectively,  $V_p = 4.5$  cm/ns and  $V_s = 7$  cm/ns. The respective velocities in frozen ground were taken from published evidence (Arcone et al., 1998; Macheret, 2006; Starovoitov, 2008): about 15 cm/ns in frozen ground and 17 cm/ns

in ice. The velocity in ice-rich peat is expected to approach that in ice. In further calculations, the velocities in frozen sand and peat were assumed to be  $V_{fs} = 15$  cm/ns and  $V_{fp} = 17$  cm/ns, respectively.

The attenuation  $\alpha$  was estimated in two ways: (i) from the amplitude of reflections from the permafrost table at different depths and (ii) from multiple waves, using only the amplitudes obtained at lithologically uniform sites (one sand site and three peat sites). We used only reflected and multiple signals free from interference with other transmitted or reflected signals. Figure 4 shows fragments of GPR data with an event of reflection from the permafrost table at a peat site. The green box frames the area used for amplitude analysis and the red one corresponds to unfit data subject to interference with transmitted signal; the panel b of Fig. 4 shows a fragment of the GPR data with a prominent multiple reflection from the permafrost table.

The suggested method only allows estimating average attenuation and is not very accurate, as the approaches to inversion (see below) neglect several factors: horizontal and vertical gradient of EM properties; frequency dependence of attenuation; source and receiver conditions; possible interference at intermediate interfaces, etc. The GPR data used for the analysis were acquired with 300 MHz antennas in air.

### Estimating attenuation from reflection amplitudes from different depths

Assuming constant EM properties on both sides of the permafrost table, the reflection amplitude according to equation (1) depends only on depth and attenuation:

$$A_h = \text{const} \cdot e^{-2h\alpha} \cdot \frac{1}{2h} \quad (3)$$

The amplitude corrected for spherical divergence depends exponentially on the double reflector depth. The equation

$$A_h \cdot 2h = \text{const} \cdot e^{-2h\alpha} \quad (4)$$

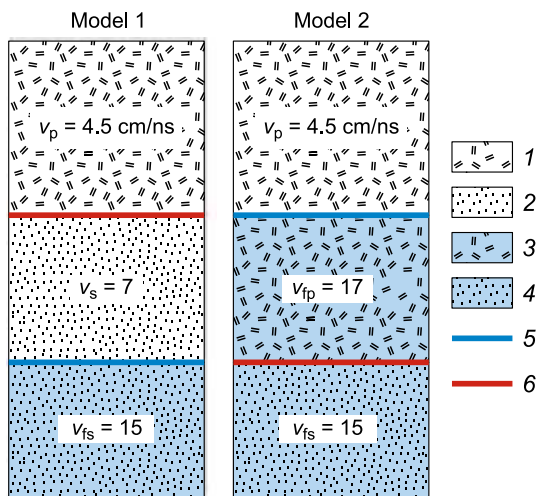
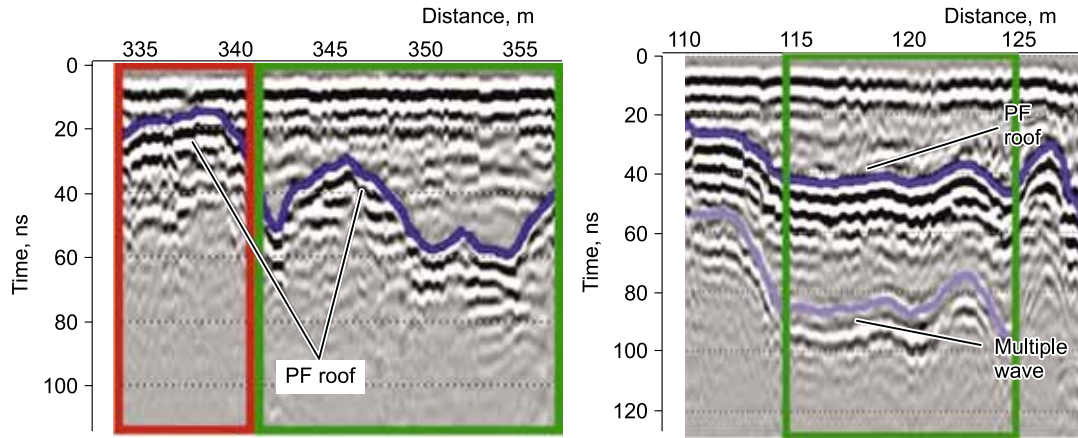


Fig. 3. Models of a peat section. Permafrost table below (Model 1) and above (Model 2) peat base. 1, peat; 2, sand; 3, frozen peat; 4, frozen sand; 5, thaw/permafrost interface; 6, peat/mineral soil interface.  $V_p$ ,  $V_s$ ,  $V_{fp}$ ,  $V_{fs}$ , velocities in thawed peat, thawed sand, frozen peat and frozen sand, respectively.



**Fig. 4.** Fragments of GPR data along profiles in peatland areas. Blue line is single reflection from permafrost table; violet line is multiple reflection from permafrost table. Red and green boxes frame, respectively, the parts of reflection with and without interference; the record free from interference was used for amplitude analysis.

is similar to  $y(x) = \text{const} \cdot e^{-x\alpha}$ , where the coefficient at  $x$  is the reflection coefficient.

The curves in Fig. 5 present the behavior of the maximum amplitude of reflection from the permafrost table corrected for spherical divergence as a function of the reflector depth for the sand (left panel) and peat (right panel) active layer, with the respective regression equations at each curve. Thus estimated attenuation values are  $\alpha = 0.42$  for sand and  $\alpha = 0.66$  for peat.

### Estimating attenuation from amplitudes of multiple reflections

Attenuation is estimated from the amplitude of multiples assuming that a multiple follows the same path as a single wave reflected from an interface (with a single arrival), but it reflects also from the ground surface and then follows the reflected path once again and reflects from an interface at some depth below the surface (Sudakova and Vladov, 2009). Correspondingly, its amplitude  $A_{2h}$  is

$$A_{2h} = A_0 K_{\text{air}} K_{\text{ref}}^2 \cdot e^{-4h\alpha} \cdot \frac{1}{4h}, \quad (5)$$

where  $K_{\text{air}}$  is the reflection coefficient from the ground surface (ground/air interface).

Therefore,

$$\alpha = \frac{\ln \left( \frac{A_h}{A_{2h}} K_{\text{air}} K_{\text{ref}} \cdot \frac{1}{2} \right)}{2h} \quad (6)$$

The attenuation  $\alpha$  was calculated from the amplitudes of multiples using the fragments of GPR data with clearly detectable reflection events free from interference with any other signal (Fig. 4b). Thus estimated attenuations are from 0.27 to 1.62 (an average of 0.8).

### Estimating total attenuation of waves transmitted through or reflected from the permafrost table

Consider the two attenuation models presented in Fig. 3. The wave either passes through the peat/soil interface and reflects from the thaw/permafrost interface (model 1) or

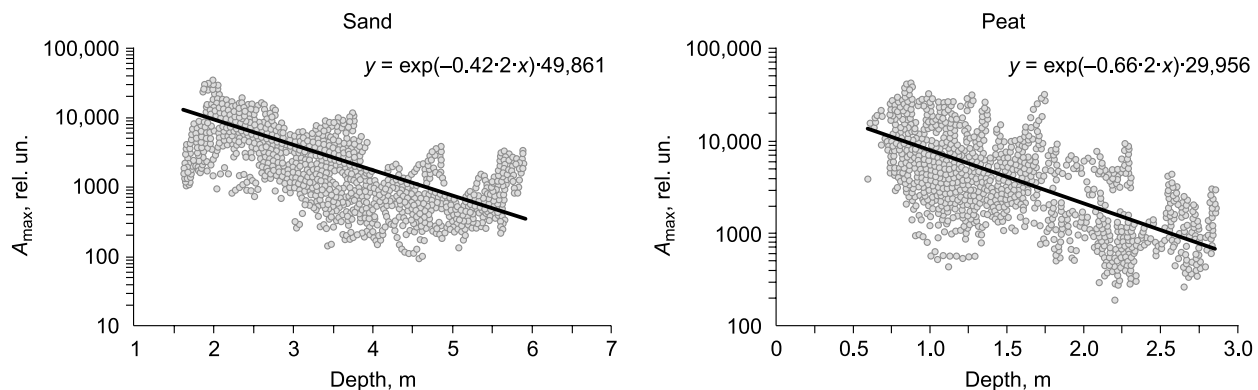


**Fig. 5.** Depth-dependent maximum amplitude of reflection from permafrost table corrected for spherical divergence, with exponential regression equations.

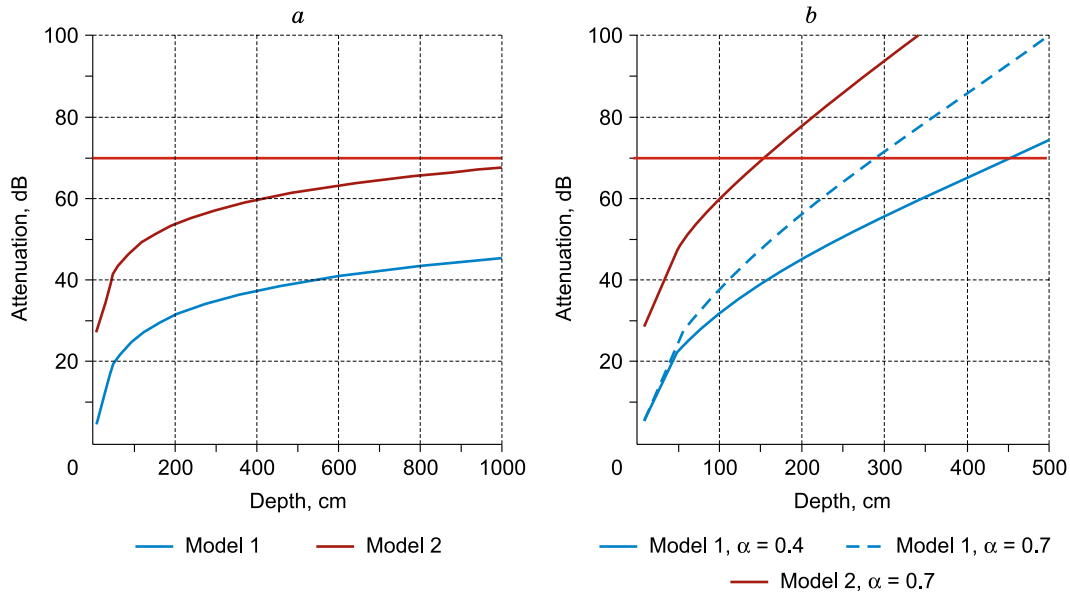


**Fig. 6.** Calculated attenuation of reflected EM waves for models 1 and 2 (Fig. 3) at different depths to permafrost, without (a) and with (b) regard to attenuation. Red line shows dynamic range.

passes through the permafrost table and reflects from the frozen peat or sand (model 2).

If the signal amplitude is 1 at a distance of 10 cm from the source, it will become 10 times weaker (0.1) at a distance of 100 cm, with regard to spherical divergence. The reflection and transmission coefficients were assumed according to velocities in Fig. 3. The reflection amplitudes were calculated by equation (1), with the attenuation  $\bar{A}$  given by

$$\bar{A} \left( \frac{\text{dB}}{\text{m}} \right) = 20 \lg \frac{A_0}{A_h}, \quad (7)$$

where  $A_0 = 1$  is the amplitude of the sounding signal (at a depth of 10 cm).

Depth-dependent attenuation is shown in Fig. 6 for the models of Fig. 3, with and without attenuation ( $\alpha = 0$ ), at the panels a and b, respectively.

Attenuation in water-saturated peat was estimated with reference to the average value over those obtained by the two above ways (0.7). In model 1, with unfrozen ground composed of water-saturated peat and sand, attenuation varies from 0.4 (all sand) to 0.7 (all peat). In model 2, attenuation in frozen ground was assumed to be zero.

The maximum penetration depth of the 70 dB radar signal differs markedly in the nonattenuating (Fig. 6a) and attenuating (b) ground: it exceeds 10 m in the former case, even when the permafrost table is above the peat base, and is 1.5 m in the attenuating ground (Fig. 6b), with the permafrost table above the mineral bed. In the latter case, no re-

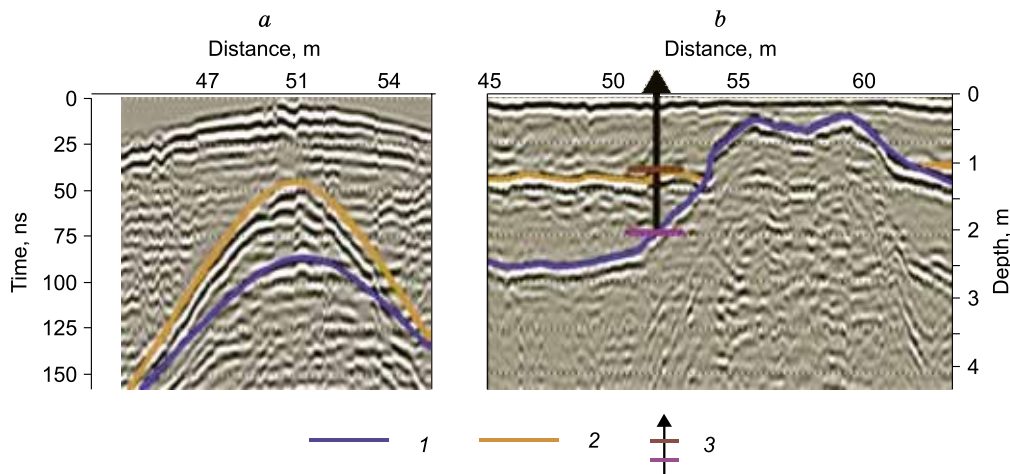


**Fig. 7.** Results of point WARR measurements (a) and continuous profiling (b). Distance points in panel (a) correspond to those in panel (b). 1, permafrost table; 2, peat base; 3, borehole with marked peat base and permafrost table.

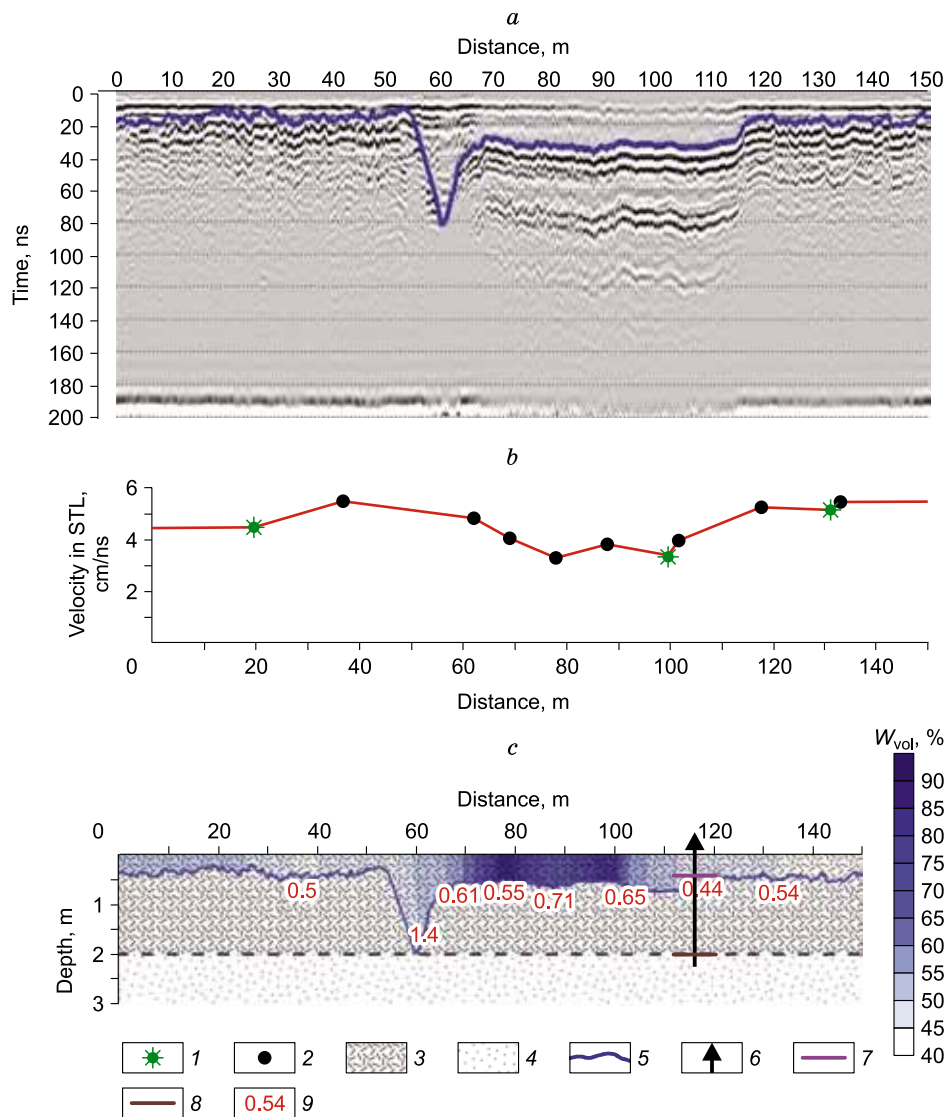


**Fig. 8.** Results of GPR surveys along profile 7: *a*, GPR data, reflection from thaw/permafrost interface; *b*, velocity in active layer along profile 7; *c*, geological cross section with volumetric water content in active layer ( $W_{vol}$ , %). 1, GPR soundings; 2, rod measurements; 3, peat; 4, sand; 5, permafrost table; 6, borehole; 7, thaw/permafrost interface from coring; 8, peat/soil interface from coring; 9, depths to permafrost (in cm) measured by rod and inferred from GPR data.

flections are resolvable below this depth. In unfrozen ground, the radar signals can penetrate 2–3 times deeper (3–4.5 m).

#### ESTIMATING DEPTHS TO REFLECTORS AND VELOCITIES FROM GPR DATA

The GPR results from a segment of profile 9 (Fig. 7) show a heterogeneous structure of the subsurface which has been confirmed by coring. The GPR data display two reflections: from the peat/soil (brown) and thaw/permafrost (blue) interfaces. The two reflectors are traceable in the time section of continuous profiling. At point 51 m, the velocities to these reflectors are, respectively, 4.3 and 5.1 cm/ns, and the depths obtained using GPR WARR measurements 105 and

220 cm, which are close to those from coring (110 and 210 cm). Thus, GPR surveys can furnish reliable constraints on velocities and depths to reflectors.

#### ESTIMATING VOLUMETRIC SOIL WATER CONTENT FROM GPR DATA

The territory of 150 m long GPR profile 5 has been characterized by three GPR soundings, data from a borehole, and thaw depth measurements with a metal rod at eight points (Fig. 8). The GPR data along the profile Fig. 8a (blue color shows reflection from the permafrost table) fails to resolve reflections from the peat/soil interface which is ~2 m deep according to coring data.

Direct measurements and GPR data provided constraints on velocities in the active layer (Fig. 8b). Two GPR points are located in the immediate vicinity from the site of active layer thickness measurements with a rod. The depths to permafrost obtained by the two methods are almost identical. The GPR velocities and the ratio of the known active layer thickness to reflection traveltimes in a zero-offset record differ for no more than 5%.

The calculated and measured velocities were interpolated between points and extrapolated linearly to the profile ends. The velocity law was used to obtain the velocity–depth model (Fig. 8c) that showed velocity variations in the active layer from 3.4 to 5.5 cm/ns. The velocity measurements allowed estimating permittivity and volumetric water content in the active layer, by the Topp's equation (Topp et al., 1980).

The soil moisture contents increase by a factor of 1.5–2 between the 70 and 110 m points. The moisture increase is also implicitly indicated by the presence of multiples from the permafrost table.

Thus, GPR profiling can, if necessary, fully or partly substitute for direct measurements of soil moisture and active layer thickness without accuracy loss.

## CONCLUSIONS

The calculations and review of field data have demonstrated that attenuation of electromagnetic waves has to be specially estimated during GPR survey planning. According to GPR profiling with a 300 MHz antenna, reflections from interfaces below the permafrost table, which is from 0 to 4–5 m deep, are detectable at an attenuation of 0.4 common to water-saturated sand. On the other hand, this fact imposes limitations on the GPR penetration depth for evaluating the amount of peat in permafrost. A possible solution may lie with winter time surveys when the active layer is fully frozen.

The depths to interfaces inferred from GPR data agree with the results of direct measurements. GPR surveys allow estimating velocities to a required resolution, which improves the accuracy of the resulting velocity and depth. Velocity variations have implications for lithological division of sections and soil moisture patterns which can be calculated using published empirical relationships. The use of GPR can reduce labor-consuming direct measurements for the active layer thickness and the properties of frozen and unfrozen ground.

The study was carried out on government assignment, as part of planned research at the Tyumen Science Center for the period 2018–2020 (protocol No. 2 of 8.12.2017). It was supported by grants 18-05-60004 from the Russian Foundation for Basic Research and 16-17-00102 from the Russian Science Foundation (for field work).

## REFERENCES

- Arcone, S.A., Lawson, D.E., Delaney, A.J., Strasser, J.C., Strasser, J.D., 1998. Ground-penetrating radar reflection profiling of groundwater and bedrock in an area of discontinuous permafrost. *Geophysics* 63, 573–584.
- Brosten, T.R., Bradford, J.H., McNamara, J.P., Gooseff, M.N., Zarnetske, J.P., Bowden, W.B., Johnston, M.E., 2009. Estimating 3D variation in active-layer thickness beneath Arctic streams using ground-penetrating radar. *J. Hydrol.* 373, 479–486.
- Butler, D.K., (Ed.), 2005. *Near-Surface Geophysics*. Society of Exploration Geophysicists. Tulsa, Oklahoma, U.S.A.
- Ermakov, A.P., Starovoitov, A.V., 2010. Use of GPR surveys for engineering geological studies of permafrost. *Bull. Moscow University* 4 (6), 91–97.
- Fotiev, S.M., 2017. Arctic peatlands of the Yamal–Gydan province of Western Siberia. *Earth's Cryosphere XXI* (5), 3–15.
- Harry, M.J. (Ed.), 2009. *Ground Penetrating Radar Theory and Applications*. Elsevier.
- Konchits, A.V., Minaeva, T.Yu. (Eds.), 2017. *Rehabilitation of Disturbed Lands Based on Ecosystem Approach: Methodological Guidelines* [in Russian]. Nariyan-Mar.
- Macheret, Yu.Ya., 2006. *GPR Surveys in Glaciers* [in Russian]. Nauchnyi Mir, Moscow.
- Malygin, P.V., Lubov, V.K., 2014. Investigation into the structure, composition and properties of peat. *Bull. Cherepovets University* 5, 12–18.
- Omeliyanenko, A.V., 2001. *GPR Surveys in Permafrost: Theoretical and Methodological Background*. Author's Abstract, Doctor Thesis (Engineering). Institute of Permafrost, Yakutsk.
- Pavlov, A.V., Malkova, G.V., 2009. Small-scale mapping of trends of the contemporary ground temperature changes in the Russian North. *Kriosfera Zemli XIII* (4), 32–39.
- Plado, J., Sibul, I., Mustasaar, M., Jõelet, A., 2011. Ground-penetrating radar study of the Rahivere peat bog, eastern Estonia. *Estonian J. Earth Sci.* 60 (1), 31–42.
- Power Economy of Russia: Strategy for the Period Till 2030, 2009. Approved by Decree 1715 of the Government of the Russian Federation, 13 November.
- Rosa, E., Larocque, M., Pellerin, S., Gagne, S., Fournier, B., 2009. Determining the number of manual measurements required to improve peat thickness estimations by ground penetrating radar. *Earth Surf. Processes Landforms* 34, 377–383.
- Sadurtdinov, M.R., Malkova, G.V., Skvortsov, A.G., Sudakova, M.S., Tsarev, A.M., 2016. The present state of sporadic permafrost in the floodplain of the Pechora River (Nenets Autonomous District): Evidence from integrate geocryological and geophysical studies, in: *Geophysical Surveys in Permafrost for Construction Purposes* [in Russian]. Proc. 5th Conf. of Russian Geocryologists. M.V. Lomonosov Moscow State University, 14–17 June 2016. *Universitetskaya Kniga, Moscow*, Vol. 1, Part 4, pp. 340–345.
- Shean, D.E., Marchant, D.R., 2010. Seismic and GPR surveys of Mullins Glacier, McMurdo Dry Valleys, Antarctica: ice thickness, internal structure and implications for surface ridge formation. *J. Glaciology* 56 (195), 48–64.
- Sjöberg, Y., Marklund, P., Pettersson, R., Lyon, S.W., 2015. Geophysical mapping of palsa peatland permafrost. *The Cryosphere* 9, 465–478.
- Starovoitov, A.V., 2008. *Interpretation of Ground Penetrating Radar Data* [in Russian]. Moscow University Press, Moscow.
- Sudakova, M.S., Vladov, M.L., 2009. Laboratory radar dielectric measurements. *Geofizika* 3, 10–19.
- Sudakova, M.S., Sadurtdinov, M.R., Malkova, G.V., Skvortsov, A.G., Tsarev, A.M., 2017. Application of ground penetrating radar in permafrost investigations. *Earth's Cryosphere XXI* (3), 69–82.

- Timofeeva, S.S., Mingaleeva, G.R., 2014. Prospects for using peat in regional power economy. *Bull. Tomsk Polytechnical University. Tekhnika i Tekhnologii v Energetike* 325 (447), 46–55.
- Topp, G.C., Davis, J.L., Annan, A.P., 1980. Electromagnetic determination of soil water content: measurements in coaxial transmission lines. *Water Resource Research* 16, 574–582.
- Vasil'chuk, Yu.K., Vasil'chuk, A.C., 2016. Thick polygonal peatlands in continuous permafrost of West Siberia. *Earth's Cryosphere XX* (4), 3–15.
- Vladov, M.L., Sudakova M.S., 2017. *Ground Penetrating Radar Surveys: from Physical Background to Prospects* [in Russian]. Geos, Moscow.

*Editorial responsibility:* M.I. Epov